PHYSICAL REVIEW E **80**, 010901(R) (2009)

Analysis of accordion DNA stretching revealed by the gold cluster ruler

Alexey K. Mazur*

Institut de Biologie Physico–Chimique, CNRS UPR 9080, 13 rue Pierre et Marie Curie, Paris 75005, France

(Received 25 January 2009; revised manuscript received 25 May 2009; published 2 July 2009)

A promising method for measuring intramolecular distances in solution uses small-angle x-ray scattering interference between gold nanocrystal labels [Mathew-Fenn *et al.*, Science **322**, 446 (2008)]. When applied to double-stranded DNA, it revealed that the DNA length fluctuations are strikingly strong and correlated over at least 80 base pair steps. In other words, the DNA behaves as accordion bellows with distant fragments stretching and shrinking concertedly. This hypothesis, however, disagrees with earlier experimental and computational observations. This Rapid Communication shows that the discrepancy can be rationalized by taking into account the cluster exclusion volume and assuming a moderate long-range repulsion between them. The long-range interaction can originate from an ion exclusion effect and cluster polarization in close proximity to the DNA surface.

DOI: 10.1103/PhysRevE.80.010901 PACS number(s): 87.14.gk, 87.15.ak, 87.15.ap, 87.15.H−

Long double-stranded DNA (dsDNA) behaves as a continuous elastic rod placed in a heat bath (Ref. [1], Chap. 19). The fluctuations of the length, L, and the end-to-end distance, R, are characterized by the canonical variances $\sigma_R^2(L)$ and $\sigma_L^2(L)$, respectively. Function $\sigma_L^2(L)$ should be linear because the stacking interactions are short range, and starting from a few base pair steps (bpss), the dsDNA can be considered as a concatenation of short independent fragments. The small-angle x-ray scattering interference (SAXSI) between gold nanocrystal labels makes possible very accurate measurements of short intramolecular distances [2]. When the length of dsDNA was measured it turned out that function $\sigma_L^2(L)$ is approximately quadratic suggesting that the length fluctuations are positively correlated over at least 80 bps [3], that is, dsDNA breathes as accordion bellows with distant fragments stretching and shrinking concertedly. This conclusion questions the current physical models of the double helix and offers a simple possibility of long-range communications along DNA, with broad mechanistic implications for gene regulation. It was argued, however [4], that the SAXSI data are not entirely consistent with earlier observations. Although the $\sigma_L^2(L)$ profile was not accurately checked before, the amplitudes of stretching fluctuations measured by other methods differ from the SAXSI results. Notably, the amplitudes of fluctuations observed in the atom force microscopy experiments [5–7] were much smaller than should be expected according to the SAXSI data [4]. The effect discovered by Mathew-Fenn *et al.* [3] probably has a different physical origin, and in the present Rapid Communication we propose an alternative interpretation of these results. We show that the striking quadratic growth of $\sigma_L^2(L)$ can be caused by the cluster-DNA excluded volume effect and weak cluster-cluster repulsion. The long-range effective repulsion between the gold labels probably results from the solvent polarization induced by the strong electrostatic field near the DNA surface.

We begin with analysis of stretching fluctuations in realistic all-atom molecular dynamics (MD) simulations of a 50-mer fragment of a poly-GC dsDNA (Fig. 1). The variance of the MD fluctuations of the DNA length can be expanded as [8]

$$\sigma_L^2(n) = nC(1) + \sum_{m=2}^{n} C(m),$$

where n is the chain length. Terms $C(m)$ include correlations of the helical rise in dinucleotides separated by $(m-1)$ steps. Term $C(1)$ is positive definite, and function $\sigma_L^2(n)$ is strictly linear when single-step fluctuations are uncorrelated along the chain [$C(m)=0$, with $m>1$]. Figure 1 reveals that stretching fluctuations at neighboring steps are anticorrelated, but the correlations fade away over about 4 bps. The $C(2)<0$ gives a small positive y intercept of the $\sigma_L^2(n)$ profile, and this is the only distinguishable deviation from strict linearity. The bending persistence length, l_b, and the stretching Young's modulus, Y_f, measured as described elsewhere [9–11] are about 100 nm and 4700 pN, respectively, indicating that the MD force field overestimates the rigidity of dsDNA [12]. To correct for this discrepancy the upper estimate of the variances in Fig. 1 should be increased by a factor of 3, and yet this gives an order of magnitude smaller values

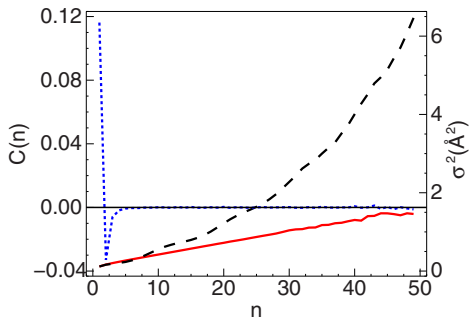

FIG. 1. (Color online) Stretching fluctuations in dsDNA according to a 208 ns of all-atom MD simulation. The left y axis and the blue dotted line show the behavior of the correlation terms $C(n)$. Variances $\sigma_L^2(n)$ and $\sigma_R^2(n)$ are shown by the solid red and dashed black lines, respectively, with the values on the right y axis. The details of MD protocols can be found elsewhere [8].

*alexey@ibpc.fr

 ©2009 The American Physical Society

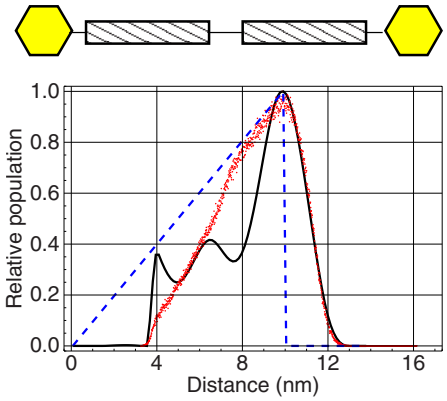

FIG. 2. (Color online) End-to-end distance distributions for the construct sketched on top. The gold nanocrystal labels and the dsDNA fragments are shown by hexagons and dashed rectangles, respectively. The distribution shown by the solid black line is constructed from the experimental data [2] by using cubic spline interpolation between several key points. The ideal theoretical distribution is shown by the dashed blue line. The dotted red trace features the results of BD simulations.

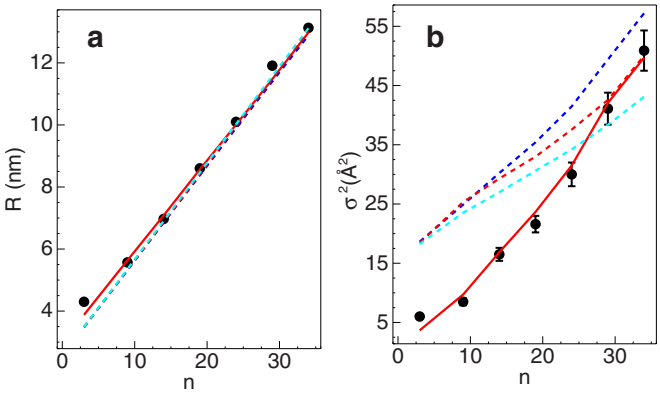

FIG. 3. (Color online) Comparison of experimental and computed (a) cluster-cluster distances and (b) distance variances. Black circles with error bars show the experimental points published in the supplement to Ref. [3]. The dashed lines show BD results for l_b=40 nm (upper blue), 50 nm (middle red), and 60 nm (lower cyan) without cluster-cluster interactions. The solid red lines correspond to l_b=50 nm with the fitted interaction potential.

than in experiment [3]. In the course of dynamics, the $C(m)$ terms with $m>4$ gradually decrease with time with the linearity of the $\sigma_L^2(n)$ plot improved. Therefore, the main features of the pattern in Fig. 1 hardly depend upon the limited MD sampling. Similar linear $\sigma_L^2(n)$ profiles were also obtained for shorter GC- and AT-alternating dsDNA [9,10].

Our MD simulations are not meant to disprove experimental observations, but they demonstrate that the most detailed dsDNA models currently used do not involve interactions that might cause long-range stretching correlations when bound to large gold nanoparticles. At the same time, the $\sigma_R^2(L)$ plot in Fig. 1 has a quadratic profile, and one can conjecture that gold cluster SAXSI measurements suffer from incomplete subtraction of the bending contribution from the measured σ_R^2. Indeed, the original interpretation [3] assumed that the labels make a constant contribution to σ_R^2, which would be true if they were freely rotating around the points of attachment. In reality, these are bulky objects that, due to the excluded volume effect, on average elongate DNA, and their contribution to $\sigma_R^2(L)$ should vary with L. The clusters are restrained by short as well as long-range interactions, and below we try to figure out under which conditions this effect can explain the gold cluster SAXSI data.

Different hypotheses were examined by using Brownian dynamics (BD) simulations with earlier tested discrete worm-like chain (WLC) models [11]. The number of beads, the link length, and the harmonic potentials were adjusted to model dsDNA fragments with l_b=50 nm and Y_f=1000 pN. The BD results are compared with experimental data for different intact double helices [3] and a hybrid construct from Ref. [2] schematically shown in Fig. 2. This construct consisted of two 12-mer dsDNA linked by a flexible hinge of three unpaired thymine bases. The polythymine single-stranded DNA (ssDNA) has a negligible bending stiffness [13]. The gold clusters were modeled as terminal beads attached by 1.5 nm flexible links with the average bend deviation angle $\bar{\theta}$=46° obtained by fitting to the experimental σ_R^2 for 35 bp dsDNA [3]. This corresponds to relatively free particles, but they never point backward with respect to the chain direction. The ssDNA was modeled by three beads joined by 0.5 nm links. The best agreement with the experimental data [2] was observed with the stiffness of the ssDNA link corresponding to a very small l_b value around 0.5 nm.

The effective diameter of a passivated gold cluster significantly exceeds that of its core. This is clearly seen from the data for the hybrid construct (see Fig. 2). Approximated as two thin rigid sticks joined by a hinge, it should give a triangular end-to-end distance distribution. The experimental distribution vanishes below 3.5 nm, which can only be due to the cluster-cluster exclusion. The contact radius of about 1.7 nm can be obtained as the radius of the nanocrystal core (0.7 nm) plus the thioglucose passivating shell (0.6 nm) plus a layer of hydration water (0.4 nm). The experimental profile in Fig. 2 features two local energy minima on the effective interaction potential, however, it is repulsive on average and apparently long range. The figure also shows the results of BD simulations of the excluded volume effect. The short-range non-neighbor interactions were modeled by a flat-bottom harmonic repulsion starting from the contact distances corresponding to DNA and cluster radii of 1 and 2 nm, respectively. The distance distribution follows the analytical form for large separations and progressively becomes depleted for distances below 8 nm where the experimental distribution exhibits a complex structure.

The experimental data for labels attached to intact dsDNA [3] are analyzed in Fig. 3. Figure 3(a) evidences that the 1.5 nm link used for attachment of the labels provides satisfactory agreement of computed and experimental DNA lengths regardless of the varied parameters. This value approximately equals the real length. Comparison of the three dashed traces in Fig. 3(b) demonstrates that the label mobility and the DNA flexibility produce a synergetic effect and increase the bending contribution to the measured σ_R^2. The bending part of the variance for 35 bp DNA with l_b

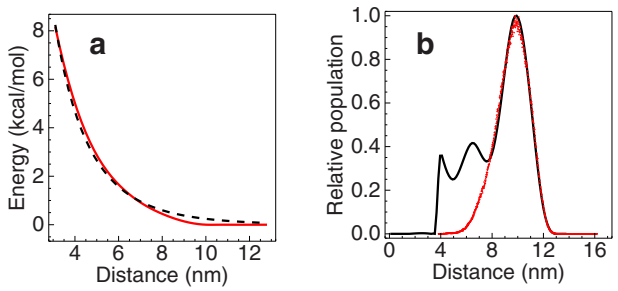

FIG. 4. (Color online) (a) The cluster-cluster interaction potential fitted to experimental data (solid red line) compared with Debye-Hückel potential with parameters given in the text (dashed black line). (b) Comparison of the experimental end-to-end distance distributions for the model system shown in Fig. 2 (solid black line) with the results of BD simulations with the fitted cluster-cluster interaction potential (dotted red line).

$=50$ nm is about 0.07 nm^2, which is less than the increment obtained by a 10 nm variation in l_b.

For short DNA the three dashed traces converge to the same variance corresponding to the distinct contribution of the cluster mobility. This value is larger than in experiment. However, in the shortest DNA fragments the labels should be significantly restrained because they almost touch one another (see Fig. 2). The effective cluster-cluster potential can be reconstructed from the experimental $\sigma_R^2(n)$ dependence in Fig. 3(b). One can reasonably assume that these interactions cease at about 10 nm. We took this point as zero, used some trial positive energy for 8 nm, and assumed that this increment doubles with the distance reduced by every 2 nm. Between these reference points the cubic spline interpolation was applied. Thus defined potential was introduced into the BD simulation algorithm and fitted by using the experimental variances. As seen in Fig. 3, the resulting discrete WLC model accurately reproduces the experimental observations.

The fitted potential is displayed in Fig. 4(a). When applied to the model system shown in Fig. 2, it reproduces the long-range peak of the distance distribution [see Fig. 4(b)]. We also checked if a similar agreement can be reached by varying only the persistence length of the central ssDNA link. With larger stiffness, this peak appears always shifted to the right and its maximum approaches the experimental position only for very small l_b of ssDNA. In the absence of the cluster-cluster repulsion, however, the distribution simultaneously acquires the shape of the dotted plot in Fig. 2 and never resembles the experimental data.

As we see, the gold cluster SAXSI data can be accounted for without hypothetical long-range stretching correlations by taking into account the exclusion volume of the reporter labels and assuming a moderate long-range repulsion between them. The origin of this repulsion is most probably electrostatic. The thioglucose shells are nominally neutral, however, the clusters have a negative charge detectable in electrophoresis [3], suggesting that the pKa of the glucose hydroxyl groups is reduced due to OH→S-Au substitution and glucose-glucose interactions at the surface. Additional repulsive forces should appear due to ion exclusion and cluster polarization in the DNA field. A hole in a dielectric exposed to external electric field can be viewed as a superposition of two oppositely polarized substances, and two such holes interact via the dipole-dipole potential. The same is true for filled holes with dielectric permittivity different from that of the media [14]. Similar qualitative considerations suggest that additional polarization equivalent to permanent Coulomb charges should result from exclusion of condensed ions from the space occupied by the clusters.

Passivated gold clusters have complex electron structures, and their dielectric properties are not known. A very high dielectric permittivity can result from delocalized electrons in the nanocrystal core, but low values are also possible if the cluster stability is due to the closed superatom electron shells similar to noble gases [15]. A rough evaluation of the possible cluster orientations near DNA shows that in both cases the induced polarization interactions should be repulsive. For an order-of-magnitude comparison we used the solution of the Poisson-Boltzmann equation for the electrostatic field around a charged sphere in an aqueous monovalent salt. The corresponding cluster-cluster interaction potential is written as (Ref. [1], Chap. 22)

$$\Phi(r) = (q^2/\varepsilon r)\exp[\kappa(a-r)]/(1+\kappa a),$$

where r is the distance, $\varepsilon=80$ is the water dielectric constant, a is the cluster radius (1.7 nm), and κ is the Debye-Hückel screening parameter (0.33 nm^{-1} in 10 mM salt). This formula gives a reasonably good agreement with the above fitted potential if the cluster charge q is about 12e [Fig. 4(a), the dashed black line]. A complete quantitative analysis of this complex system requires additional studies including accurate treatment of the finite particle size, multipole interactions, and electrostatic saturation. Nevertheless, Fig. 4(a) demonstrates that the experimental data are reproduced with reasonable interaction energies.

Our interpretation suggests that, in close proximity to the DNA surface, the electrostatic screening along its axis is not described by the Debye-Hückel theory. The experimental distance variances are similar under 10 mM, 100 mM, and 1 M NaCl [3], which was interpreted as the absence of electrostatic interactions, but in fact proves only the absence of strong salt dependence in both the bending DNA stiffness and the cluster-cluster interactions. The first assertion agrees with some earlier experimental data [16,17]. The environment of the double helix strongly differs from the average solution conditions, notably, the local ion concentration near DNA is higher than 1 M regardless of the net amount of the added salt. The cluster-cluster interactions occur through DNA and the condensed ion layer, which does not correspond to the classical Debye-Hückel screening. The long-range repulsion might not change significantly with the NaCl concentrations used in experiments [2,3]. In agreement with this assumption, the interaction potential fitted to the data collected in 100 mM NaCl (Fig. 3) appears applicable to the distance distribution obtained in 1M NaCl [Fig. 4(b)].

The foregoing analysis and the proposed alternative interpretation of the experimental data involve strong assumptions that require further verification. However, these assumptions are physically reasonable and they do not contradict the available data, in contrast to the original hypothesis of accordion stretching correlations in the DNA

double helix [4]. If this mechanism is confirmed, the gold cluster SAXSI would present a promising tool for probing electric fields near DNA and other polyelectrolyte surfaces. Effective particle-particle interactions due to solvent polarization around the double helix are important, for instance, for association of multiprotein complexes on DNA. Additional insights in these interactions can be obtained by direct atomistic MD simulations. This work is now in progress.

[1] C. R. Cantor and P. R. Schimmel, *Biophysical Chemistry* (W. H. Freeman, San Francisco, 1980).
[2] R. S. Mathew-Fenn, R. Das, J. A. Silverman, P. A. Walker, and P. A. B. Harbury, PLoS One **3**, e3229 (2008).
[3] R. S. Mathew-Fenn, R. Das, and P. A. B. Harbury, Science **322**, 446 (2008).
[4] A. K. Mazur, e-print arXiv:0904.2678.
[5] C. Rivetti and S. Codeluppi, Ultramicroscopy **87**, 55 (2000).
[6] A. Sanchez-Sevilla, J. Thimonier, M. Marilley, J. Rocca-Serra, and J. Barbet, Ultramicroscopy **92**, 151 (2002).
[7] A. Podesta, L. Imperadori, W. Colnaghi, L. Finzi, P. Milani, and D. Dunlap, J. Microscopy (Oxford) **215**, 236 (2004).
[8] See EPAPS Document No. E-PLEEE8-80-R04907 for auxiliary derivations and details of simulation protocols. For more information on EPAPS, see http://www.aip.org/pubservs/epaps.html.
[9] A. K. Mazur, Biophys. J. **91**, 4507 (2006).
[10] A. K. Mazur, J. Phys. Chem. B **113**, 2077 (2009).
[11] A. K. Mazur, J. Phys. Chem. B **112**, 4975 (2008).
[12] The Y_f value is two times larger than in the earlier study [9] because a different method was used for analysis of DNA structures.
[13] N. L. Goddard, G. Bonnet, O. Krichevsky, and A. Libchaber, Phys. Rev. Lett. **85**, 2400 (2000).
[14] C. J. F. Böttcher, *Theory of Electric Polarization: Dielectrics in Static Fields* (Elsevier, Amsterdam, 1973), Vol. 1.
[15] M. Walter, J. Akola, O. Lopez-Acevedo, P. D. Jadzinsky, G. Calero, C. J. Ackerson, R. L. Whetten, H. Gronbeck, and H. Hakkinen, Proc. Natl. Acad. Sci. U.S.A. **105**, 9157 (2008).
[16] P. J. Hagerman, Annu. Rev. Biophys. Biophys. Chem. **17**, 265 (1988).
[17] C. G. Baumann, S. B. Smith, V. A. Bloomfield, and C. Bustamante, Proc. Natl. Acad. Sci. U.S.A. **94**, 6185 (1997).